Mix Sustentável

Evaluation of biochar from banana peel pyrolysis for agricultural soil applications

Avaliação do biocarvão proveniente da pirólise da casca de banana para aplicações em solos agrícolas

Evaluación del biocarbón proveniente de la pirólisis de la cáscara de plátano para aplicaciones en suelos agrícolas

Guilherme Bampi Righetto[1]
Regina Célia Espinosa Modolo[2]
Rodolfo Rodrigues[3]
Paulo Roberto Wander[4]
Carlos Alberto Mendes Moraes Moraes[2]

[1] UniSATC - Centro Universitário UniSATC, Brasil
[2] UNISINOS - Universidade do Vale do Rio dos Sinos, Brasil
[3] UFSM - Universidade Federal de Santa Maria, Brasil
[4] UFRGS - Universidade Federal do Rio Grande do Sul, Brasil

Correspondence to: righetogbr@gmail.com

Abstract: This research evaluated the characteristics of biochar produced from slow pyrolysis of banana peel for agricultural soil applications. Two operating conditions were used with a pyrolysis temperature of 370 °C and heating rates of 11 °C/min and 35 °C/min. These conditions were determined with the aid of a computer model using Chemkin software. Pyrolysis products were characterized with respect to potential of hydrogen (pH), electric conductivity (EC), cation

ORIGINAL ARTICLE - SCIENTIFIC SECTION

Responsible editors: Lisiane Ilha Librelotto, Dr. Eng., Paulo Cesar Machado Ferroli, Dr. Eng.

Submitted on
26/11/2025
Accepted on
26/12/2025
Published on
31/03/2026

PID
110.29183/2447-3073.MIX2025.v11.n2.162-184

exchange capacity (CEC), morphology, surface area, C/N, H/C and O/C atomic ratios. Results showed an alkaline structure with a pH of 12.60 and CEC of 511 mmol/kg – suitable for soil amendment. The increase in the pyrolysis heating rate resulted in higher stability of the biochar due to the low H:C atomic ratios while increases in surface area and the number of pores was evident. Overall, the characteristics found in the produced biochars demonstrated viable application in agricultural soils as amendment.

Keywords: Banana peel; Biochar; Agricultural soil; Thermochemical conversion simulation; Agricultural waste.

Resumo: Esta pesquisa avaliou as características do biochar produzido a partir da pirólise lenta da casca de banana para aplicações em solos agrícolas. Foram utilizadas duas condições de operação com temperatura de pirólise de 370 °C e taxas de aquecimento de 11 °C/min e 35 °C/min. Essas condições foram determinadas com o auxílio de um modelo computacional utilizando o software Chemkin. Os produtos da pirólise foram caracterizados quanto ao potencial de hidrogênio (pH), condutividade elétrica (CE), capacidade de troca catiônica (CTC), morfologia, área superficial, relações atômicas C/N, H/C e O/C. Os resultados mostraram uma estrutura alcalina com pH de 12,60 e CTC de 511 mmol/kg – adequada para correção de solo. O aumento na taxa de aquecimento da pirólise resultou em maior estabilidade do biochar devido às baixas razões atômicas H:C, enquanto aumentos na área superficial e no número de poros eram evidentes. No geral, as características encontradas nos biochars produzidos demonstraram aplicação viável em solos agrícolas como corretivo.

Palavras-chave: Casca de banana; Biocarvão; Solo agrícola; Simulação de conversão termoquímica; Agricultural waste.

Resumen: Esta investigación evaluó las características del biocarbón producido a partir de la pirólisis lenta de la cáscara de plátano para aplicaciones en suelos agrícolas. Se utilizaron dos condiciones de operación con una temperatura de pirólisis de 370 °C y tasas de calentamiento de 11 °C/min y 35 °C/min. Estas condiciones fueron determinadas con la ayuda de un modelo computacional utilizando el software Chemkin. Los productos de la pirólisis fueron caracterizados en cuanto al potencial de hidrógeno (pH), conductividad eléctrica (CE), capacidad de intercambio catiónico (CIC), morfología, área superficial y relaciones atómicas C/N, H/C y O/C. Los resultados mostraron una estructura alcalina con pH de 12,60 y CIC de 511 mmol/kg, adecuada para la corrección del suelo. El

Author Contributions according to the CRediT Taxonomy

GBR: Conceptualization, Data curation, Methodology, Project administration, Validating, Visualization, Writing – original draft and Writing – review & editing. RCEM: Conceptualization, Methodology, Project administration, Supervision, Validating and Writing – review & editing. RR: Software, Validating and Writing – review & editing. PRW: Methodology, Software, Validating and Writing – review & editing CAMM: Validating and Review.

Conflict declaration

Nothing to declare.

Funding source

This study was financed in part by the Brazilian agencies CNPq and CAPES.

aumento en la tasa de calentamiento de la pirólisis resultó en una mayor estabilidad del biocarbón debido a las bajas razones atómicas H:C, mientras que los incrementos en el área superficial y en el número de poros eran evidentes. En general, las características encontradas en los biocarbones producidos demostraron una aplicación viable en suelos agrícolas como enmienda.

Palabras clave: Cáscara de plátano; Biocarbón; Suelo agrícola; Simulación de conversión termoquímica; Residuos agrícolas.

How to cite this article: RIGHETTO, Guilherme Bampi; MODOLO, Regina Célia Espinosa; RODRIGUES, Rodolfo; WANDER, Paulo Roberto; MORAES, Carlos Alberto Mendes Moraes. Evaluation of biochar from banana peel pyrolysis for agricultural soil applications. **Mix Sustentável**, Florianópolis, v. 11, n. 2, p. 162-184, 2025. DOI: http://dx.doi.org/10.29183/2447-3073.MIX2025.v11.n2.162-184.

1 INTRODUCTION

The banana is one of the most widely consumed fruits. Regardless of the inaccuracies in data collecting due to many small and informal producers, the World-wide cultivation has been estimated at 5.4 million hectares and 114 million tons yearly (Loo; Koppejan, 2008; Shiung *et al.*, 2018). In general, 30% to 40% of fruit farming yields are lost during picking and post-processing (Ali *et al.*, 2019; Bediako *et al.*, 2019). Consequently, a large amount of biowaste is generated from banana production and consumption, creating additional issues to waste management (Ali *et al.*, 2019; Souza *et al.*, 2012). Banana peels from industrial/domestic consumption and production are generally disposed-off to landfills. Due to the large volume generated, the thermochemical treatment of this biomass is under consideration to convert it into a more stable and valuable resource. The technological, environmental and economic enhancement of the converted biomass lies on several uses it achieves after conversion, such as energy generation, methane and hydrogen production from hydrolysis, effluent treatment, soil amendment, carbon capture and others (Ali *et al.*, 2019; Bediako *et al.*, 2019; Loo; Koppejan, 2008; Nathoa; Sirisukpoca; Pisutpaisal, 2014; Shiung *et al.*, 2018; Souza *et al.*, 2012).

Biochar, in general, is produced through slow pyrolysis with heating rates from 1 °C/min to 20 °C/min and typical temperatures between 350 °C and 700 °C (Bruckman *et al.*, 2016; Novotny *et al.*, 2015; Ok *et al.*, 2015; Ralebitso-senior; Orr, 2016). Final biochar properties can be adjusted with changes to pyrolysis parameters such as: temperature, heating rate, residence time and type of biomass. Higher temperatures (above 550 °C) result in more stable aromatic biochars with large specific surface areas (above 400 m^2/g). In contrast, lower temperatures reduce production costs but result in less condensed and more biodegradable structures (Basu, 2008; Bruckman *et al.*, 2016).

Regarding the soil amendment, studies have been conducted to develop specific biochars to address issues in the upper soil layers (depths from 0 cm to 40 cm). These issues range from excessive salinity, erosion, nutrient depletion from intensive agricultural practices, acidity, toxic metallic ion and agrichemical contamination, which reduces micro bacterial soil activity and yield (Meena, 2020). A further advantage of biochar application is carbon sequestration in the soil, which reduces CO_2 presence in the atmosphere and partially replaces simple fertilizers in crops (Ok *et al.*, 2015; Ralebitso-senior; Orr, 2016). Consequently, there is an emerging potential of a biochar-based agricultural circle. Some of the advantages of using biochar can be found in increased yields (through micro bacterial stimulation in the rhizosphere), lower total energy consumption (through less demand for fertilizers), lower carbon emissions (through carbon sequestration) and lower irrigation demand (through increases in soil water retention) (Bruckman *et al.*, 2016; Ok *et al.*, 2015; Ralebitso-senior; Orr, 2016; Singh; Camps-arbestain; Lehmann, 2017). Banana peels, due to their large production/ consumption and environmental and economic impact, are a conveniently suitable source material with technological, environmental, and economic enhancement. In this current study, the agricultural applications of biochar obtained from the slow pyrolysis of banana peels have been evaluated with the help of computational tools to assess the influence of operating conditions (temperature, heating rate and residence time) during the pyrolysis process.

2 METHODOLOGY

This research was performed in four steps:

1. Processing and characterization of fresh biomass.
2. Development of a slow pyrolysis heating profile through computational modelling and comparison with literature data and experimental results from a bench-scale reactor.
3. Characterization of biochar produced in the bench-scale reactor of step 2.
4. Analysis of properties obtained from step 3 and correlation with desired characteristics for soil amendment.

2.1 Biomass and biochar characterization

The biomass used in the experiments was peels of Dwarf Brazilian bananas/Prata (Musa brasiliensis) of the AAB group, Pome subgroup, produced in southern Brazil. The banana samples were obtained from commercial suppliers in the city of Canoas, Rio Grande do Sul, in maturity stage 7. This maturity scale follows the nomenclature and peel characteristics set by Emaga et al. (Emaga *et al.*, 2007). The banana samples were obtained from the complete separation of the fruit from the peel and stem, which were then dried for 24 h at a temperature of 105 ºC ± 2 ºC. Dried samples were chopped in a food processor and further ground in a pestle until particle dimensions were less than 1 mm for characterization. For biochar production, particle diameters were kept between 3.35 mm and 4.75 mm.

Raw peels were subjected to a thermogravimetric (Perkin Elmer TGA/DTG analyzer, model STA 8000) and heating value (IKA Calorimeter, model C-200) analyses in accordance with ASTM E 711 (ASTM, 2004). Dry peel and biochar specific surface areas were determined by the Brunauer-Emmett-Teller method (MICROMERITICS analyzer, model Tristar Plus II) and bulk densities were measured with a Helium gas pycnometer (model AccuPyc II 1340). Ultimate analyses of the dry peel and biochar samples were conducted with the Pregl–Dumas method (Elemental/Vario MACRO Cube analyzer). A TGA analysis was performed on the dry peel with a NAVAS analyzer model TGA-1000 in accordance to the procedures of (Cassel, n.d.), in order to carry out the proximate analyses. Dry peel and biochar pH and electrical conductivity were analyzed with normative procedures in IN 17 from "Secretaria de Defesa Agropecuária do Brasil" (Brasil, 2007) with a DM-20 pH meter and DM-31 EC meter, respectively. Additionally, biochar was tested for cation exchange capacity (CEC) also following procedures from IN 17. Finally, biochar morphology was determined from scanning electron microscopy (SEM) with an EVO MA15-Zeiss microscope.

2.2 Computational Model

The solid fraction obtained from a pyrolysis process is affected by several operating conditions such as temperature, residence time and heating rate. To obtain a range of estimated products (biochar, bio-oil, gas) from the thermochemical conversion, the computational model of Debiagi *et al.* (2018) was used. This model suggests that a biomass can be described from a linear combination of primary structures: cellulose (CELL), hemicellulose (HCELL), lignin (LIG-C, LIG-H and LIG-O) and extractives (TANN and TGL). The predicted biomass composition must only comply with C, H and O atomic balances so five degrees of freedom lead to five division parameters (α, β, γ, δ and ε). These parameters define three reference mixtures (RM- 1, RM-2 and RM-3) representative of the concentrations obtained from those three chemical elements. From these mixtures, CELL, HCELL, LIG-C, LIG-H, LIG-O, TANN and TGL biomass quantities can be estimated. The calculated fraction of each primary structure in the biomass samples were inserted in ANSYS CHEMKIN© 2020 R1 version with chemical kinetics and thermodynamic data from (Debiagi *et al.*, 2018). Other input data were temperature profile, pressure, physical characteristics, and reactor type, in this case a Closed Homogeneous Batch Reactor. The simulated operating conditions for critical variables are shown in Tab. 1.

Table 1 – Operating conditions used in ANSYS CHEMKIN© to simulate biochar production.

Variable	**Temperature (°C)**	**Heating rate (°C/min)**
Tested values	250, 260, 270, 280, 290, 300, 310, 320, 330, 340, 350, 360, 370, 380, 390, 400, 410, 420, 430, 440, 450, 460, 470, 480, 490, 500, 510, 520, 530, 540, 550, 560, 570, 580, 590 and 600.	2, 4, 6, 8, 10, 12, 14, 16, 18, 20, 22, 24, 26, 28 and 30.
Time	300 min at each selected temperature	

Source: The Authors.

Simulation parameters were:

1. Problem type: constant pressure and temperature;
2. Simulation time: 300 min at each temperature;
3. Reactor wall: defined to be at the same temperature as the biomass;
4. Pressure: defined as 1 atm for the system;
5. Biomass composition: considered in terms of the mass of each component of its structure and normalized by the software.

2.3 Biochar production

Pyrolysis of the banana peel was performed in a bench- scale furnace. The furnace is equipped with a tubular horizontal quartz reactor as well as a programmable logic controller, which allows the control of time, temperature and heating rate of the pyrolysis process. A flow meter allows a constant inflow of N_2 to prevent biomass oxidation from contact with atmospheric air and to carry pyrolysis gases away from the pyrolysis zone.

Results from the computation model were compared to literature data (Ali *et al.*, 2019) to determine pyrolysis temperature, heating rate and biochar residence time for two experimental runs. Each run contained a 40 g sample and particle sizes range 3.35 to 4.75 mm. The placement of the biomass samples in the reactor was such that they completely covered the thermocouple, and the inner channel surface was in contact with the external biomass layer. Permanent gases and condensable vapors were not considered in the analysis and were consequently discarded. Biochar from the first run was labeled “A” and from the second one was called “B.”

3 RESULTS AND DISCUSSION

3.1 Physicochemical characteristics of fresh banana peel Thermal decomposition of dry biomass

Measured mass fractions of C, H, O, N and S were coherent with reference values. As shown in Tab. 2, C and O were the most common species with 48.13% and 44.73%, respectively. The measured amount of C (48.13%) was larger than one obtained for banana peels in other studies, which varied from 35.65% to 45.89% (Bediako *et al.*, 2019; Omulo *et al.*, 2019; Tahir *et al.*, 2019) and also other agricultural biomasses (47.40%) (Vassilev et al., 2010). Proximate analysis of the fresh banana peel found a high moisture content (88.67%, db) and volatile matter content (75.29%wt, db), which is a value expected in common biomasses. Ash content was measured as 15.65%, db, which is higher than found in other studies (Leobet, 2016; Omulo *et al.*, 2019; Tahir *et al.*, 2019) and average agricultural biomasses (Vassilev *et al.*, 2010), which indicates a higher mineral concentration (Loo; Koppejan, 2008). The amount of fixed carbon was low (8.77% db) compared to other studies (20.55% and 26.12%) using the same type of biomass (Leobet, 2016; Tahir *et al.*, 2019), and (19.10%) compared to average agricultural biomasses (Vassilev *et al.*, 2010). This indicated fast devolatilisation during conversion and the potential to produce highly reactive gaseous fuels (Tahir *et al.*, 2019). Higher heating value was measured as 18.91 MJ/kg, in line with other biomasses such as wheat straw (16.79 MJ/ kg), cork pellets (19.38 MJ/kg), sunflower husks (20.28 MJ/ kg), cotton residue (16.65 MJ/kg) and soy residue (18.77 MJ/kg). This result indicated a similar potential in energy generation (Motghare *et al.*, 2016; Naydenova *et al.*, 2020).

Table 2 – Fresh banana peel characteristics.

Proximate analysis (%wt dry basis, except moisture)	
Moisture	88.67
Volatile Matter	75.29
Ash	15.65
Fixed Carbon	8.77
Ultimate analysis (%wt dry basis)	
C	48.13
H	5.79
O*	44.73
N	1.21
S	0.14
Higher heating value (MJ/kg)	18.91

*Determined by difference.

Source: The Authors.

Fig. 1 shows the TG and DTG curves of dry banana peel samples. The experiment was performed at a temperature range from 25 to 950 °C in an inert N_2 environment. Losses that occur up to 160 °C are related both to free and bound water, followed by extractives at around 220 °C. Three well defined exothermal peaks can be observed. The first peak at 254 °C is related to the decomposition of less stable biomass structures such as hemicellulose. The second peak at around 304 °C corresponds to a larger mass loss related to the cellulose decomposition. The third peak at around 400 °C corresponds to the decomposition of the remaining structures such as lignin.

Other studies on banana peel, such as (Tahir *et al.*, 2019), determined a single peak at 309 °C for the combined decomposition of cellulose and hemicellulose in the biomass structure at temperatures ranging from 163 to 386 °C. In the same study the lignin peak occurred at a higher temperature of 485 °C which was nonetheless still within the range 386 to 650 °C of structural decomposition of most lignocellulosic biomasses (Tahir *et al.*, 2019).

3.2 Model validation

From the prediction model the following mass (Tab. 3) fractions were obtained.

Table 3 – Predicted values of the primary structures.

CELL	**HCELL**	**LIGC**	**LIGH**	**LIGO**	**TGL**	**TANN**
0.2269	0.1513	0.092	0.366	0.002	0.1607	0.0006

Source: The Authors.

Results from the simulated decomposition are shown in Fig. 2a-d for cellulose (CELL and CELLA), hemicellulose (XYGR, HCE1 and HCE2), lignin (LIGC, LIGH, LIGO, LIG, LIGOH and LIGCC) and extrac-

Figure 1 – TGA/DTG of dry banana peels.

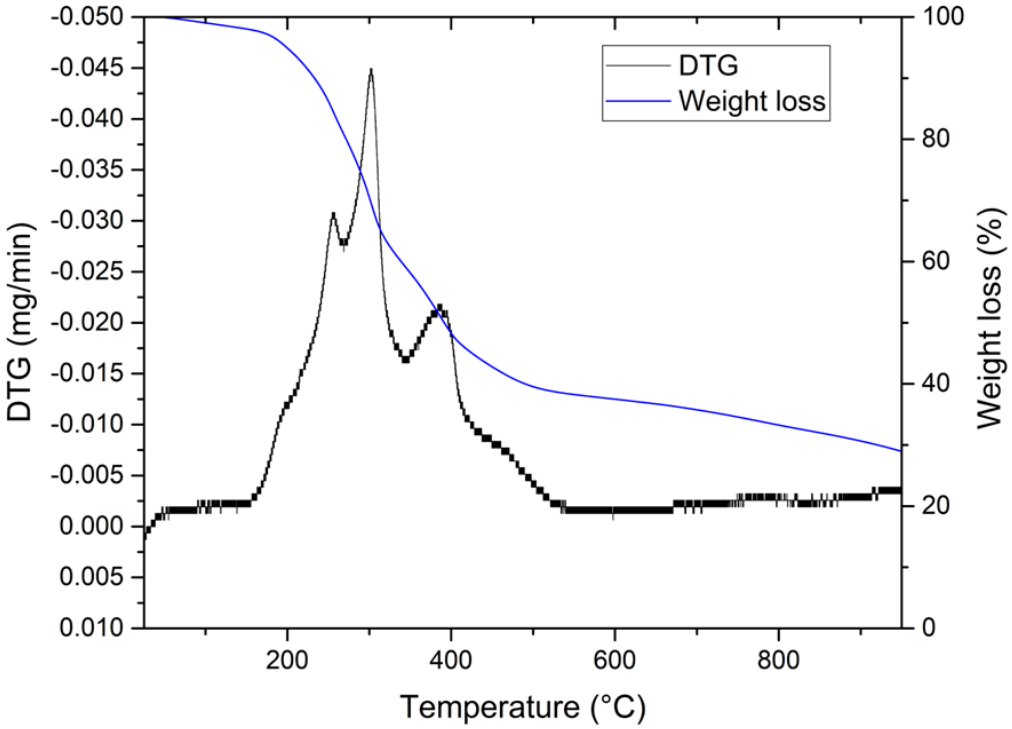

Source: The Authors.

tives (TGL, TANN and ITANN) structures. All structures present a delay in breakdown until around 200 °C is reached and breakdown starts. In the case of cellulose, thermochemical reactions only reach energy levels sufficient to trigger product formation around 204 °C. This is followed by a large mass change from approximately 300 to 400 °C, at which temperature the cellulose has been completely decomposed.

Hemicellulose, the least stable structure in the biomass, starts decomposing into intermediate reactants XYGR, HCE1 and HCE2 at around 117 °C with little mass losses. At around 200 °C, break down into HCE1 and HCE2 occurs, which in turn decompose completely above 300 °C. This behavior was explained in (Chen *et al.*, 2018) with the mass losses in a first peak attributed to cleaving of glycosidic bonds and lateral chain decomposition, while a second peak was related to monosaccharide fragmentation. The first peak is well defined in Fig. 3 from 200 to 300 °C indicating good agreement between the simulation models.

As noted in (Eduardo *et al.*, 2015), lignin breaks down into LIGC, LIGH, LIGO, LIG, LIGOH and LIGCC. Due to the sheer number of structures, a large range of decomposition temperatures is to be expected. As seen in Fig. 2c, a small mass variation starts around 150 °C mainly due to LIGO degradation and further variations extend all the way to 600 °C. Overall, the simulated decomposition profile of lignin agrees with most lignocellulosic biomasses, which occur from 150 to 1,000 °C (Branca; Blasi, 2015; Bruckman *et al.*, 2016). TANN and ITANN extractives are found to be less than 1% w.t. and decompose at low temperatures of around 100 °C. Although their direct product is biochar, their low concentrations present a negligible presence in Fig. 2d. On the other hand, TGL extractive has much higher activation energy so that its decomposition occurs at much higher temperatures, above 400 °C.

Fig. 2e-f presents a comparison of DTG curves and weight loss between simulated values and experimental data. This comparative allows an overview of temperature ranges in which the largest weight loss occurs due to the primary structures' degradation. DTG peaks are shifted towards higher temperatures due to the delay in the start of breakdown until 200 °C. However, the temperature difference is of 50 °C between results, with the peak in cellulose degradation occurring at 300 °C in the experiment and 370 °C in the simulation. This temperature difference indicates possible discrepancies in the final product, more specifically in range 200 °C to 400 °C as shown in Fig. 2f. Within this range, an overestimation of as much as 20% in mass fraction of solid products may occur in the simulation. Consequently, it is preferable that temperatures close to or above 400 °C should be used in the pyrolysis process to reconcile simulation and real biomass behavior.

3.3 Effect of temperature, heating rate and heating time in the pyrolysis products

Fig. 3a presents simulation results on the effect of temperature on solid pyrolysis products from 250 to 590 °C. The solid products are considered to be the sum of all primary structures not yet decomposed namely, pyrogenic carbon and solid metaplastic species (Eduardo et al., 2015). Under this definition, all curves show a tendency of decreasing total solids as temperature increases. For example, after 300 min at 270 °C, 64% of total solids remain, but at 590 °C, only 22% of them remain.

Relative changes in pyrolysis products yield tend to increase with temperatures range 250 to 350 °C, with a decrease of up to 10% for a 20 °C temperature increase. Above 370 °C, the curves tend to flatten out, resulting in changes of less than 1% in products yield for the same temperature increases. This trend agrees with previous results considering that larger mass decompositions were found below this temperature range.

From a pyrolysis product yield perspective, lower temperatures are desired since they result in a larger converted amount of biochar. On the other hand, higher temperatures are desirable for potentially generate biochar with larger surface area, pH, cation-exchange capacity and, consequently, more active functional groups to interact with the soil (Ok *et al.*, 2015). This trend was also observed in (Ali *et al.*, 2019), where pyrolysis at 350 °C and a heating rate of 7 °C/min resulted in a biochar that stimulated soil microbial cultures and increased chemical oxygen demand (COD) and nitrogen in the soil. Consequently, a reactor temperature of 370 °C was selected for this study to maintain a favorable pyrolysis product yield while decreasing the discrepancy between the simulation and experimental data noted in Sec. 3.2.

Fig. 3b presents total solid curves with respect to the heating rates listed in Tab. 2 (from 2 °C/min to 30 °C/min by 2 °C/min increments) at 370 °C and 300 min of heating time. An inverse proportional relation is observed between the heating rate and total solid pyrolysis yield: as heating rate increases, less biochar is obtained. However, the relative change in yield is small (less than 1% for each 2 °C/min increase) and further decreases as heating rate increases. It should be noted that higher heating rates lead to less heating and oven operational time, which would result in a reduction in energy demand. On the other hand, increases in heating rate bring about an increase in power demand. For this study, a higher heating rate was chosen due to the low relative change in solid product yield and lower heating time.

Figure 2 – Simulated results of (a) cellulose decomposition; (b) hemicelullose decomposition; (c) lignins decomposition; (d) extractives decomposition; (e) DTG comparison between simulation and experiment; and (f) weight loss behaviour of simulation and experiment.

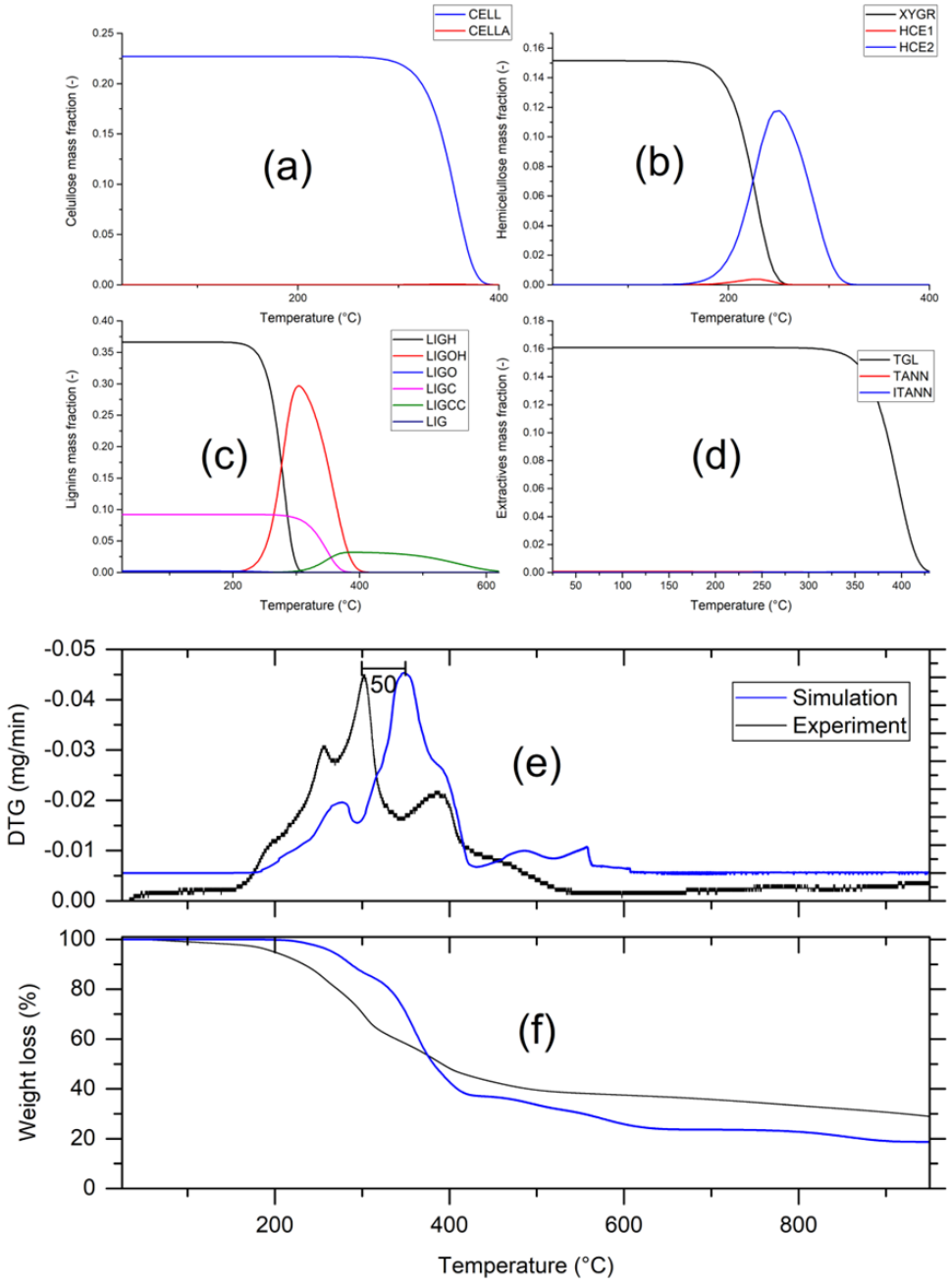

Source: The Authors.

Figure 3 – (a) Effect of temperature on overall solid pyrolysis products; (b) simulation results of heating rate on total solids for pyrolysis at 370 °C.

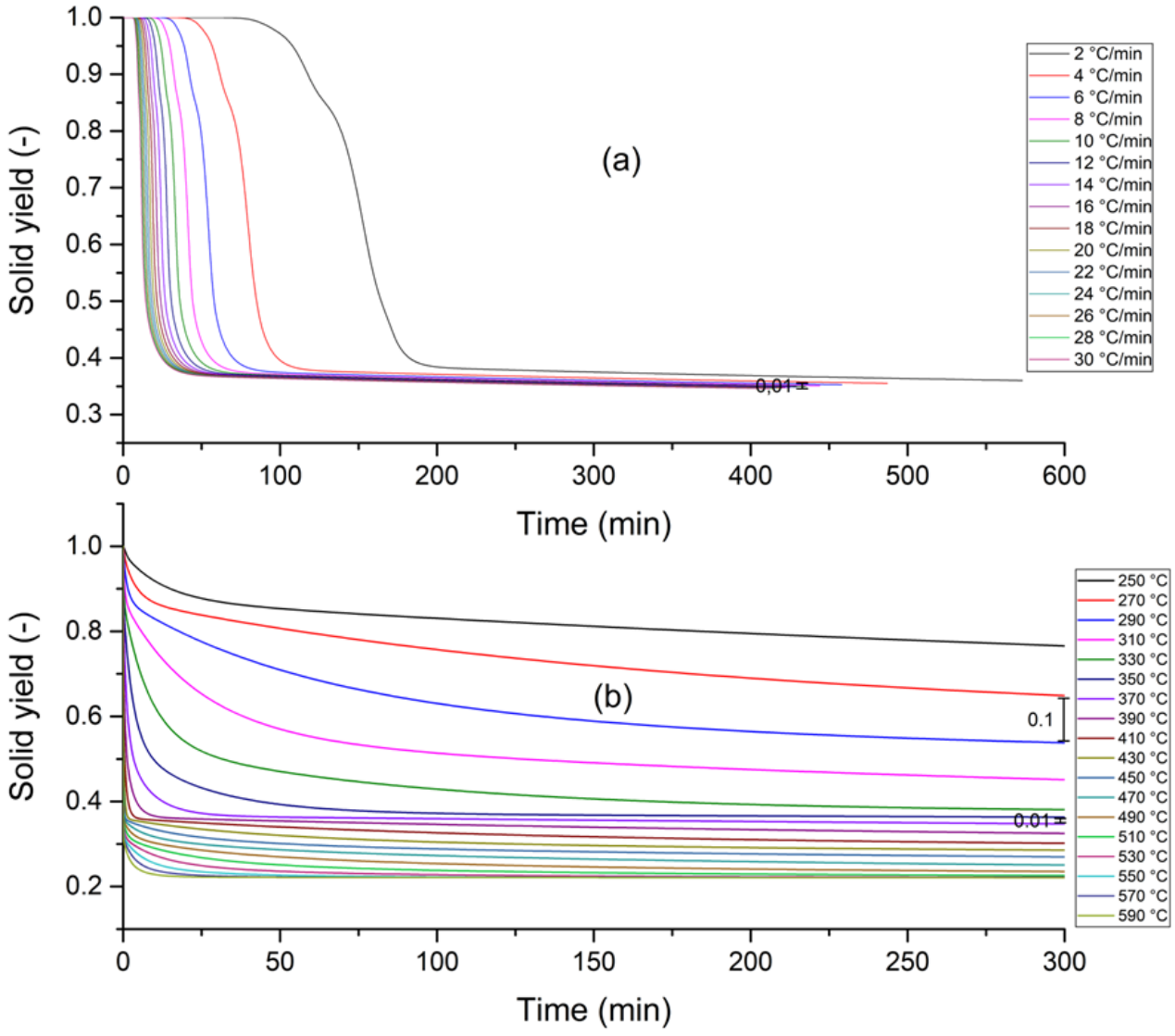

Source: The Authors.

Fig. 4a-b shows the thermal decomposition of the two simulated heating profiles selected based on their effect on primary structures. For a heating rate of 11 °C/min shown in Fig. 4a, the biomass reaches 370 °C in 31 min and primary structures are decomposed after 50 min from the start of the process, except for LIGCC which remained stable until the end of the simulation time. In contrast, the heating rate of 35 °C/min shown in Fig. 4b breaks down primary structures faster, approximately 10 min after reaching 370 °C. Sharper gradients can be observed for all species and total conversion into products is reached after an additional 30 min of heating. These results suggested a heating time of 30 min for the experiments is adequate to ensure that all structures would be converted into biochar and other pyrolysis products. Fig. 4c shows the major pyrolysis products from the two simulated heating rates of Fig. 4a-b (11 °C/min and 35 °C/min). Most solid products were in the form of CHAR (pyrogenic carbon) and metaplastic species ($GCOH_2$ and GCH_2O). Most prevalent chemical species were MLINO and $C_6H_{10}O_5$ and gases such as CO_2, CO and water. The main difference between the two heating rates is the fraction of solids generated at the end of conversion. The lower heating rate of 11 °C/min resulted in a pyrolysis product yield of 36.91% while the higher heating rate of 35 °C/min resulted in 35.63%. The higher pyrolysis product yield at 11 °C/min was expected based on previous results, however, at 35 °C/min, a slightly larger amount of CHAR was generated (less than +1%) which suggested that higher heating rates might increase pyrogenic carbon generation.

Figure 4 – (a) Simulation results of biomass primary structures breakdown for heating rates of 11 °C/min; (b) 35 °C/min; and (c) Simulation results of pyrolysis products with respect to heating rate.

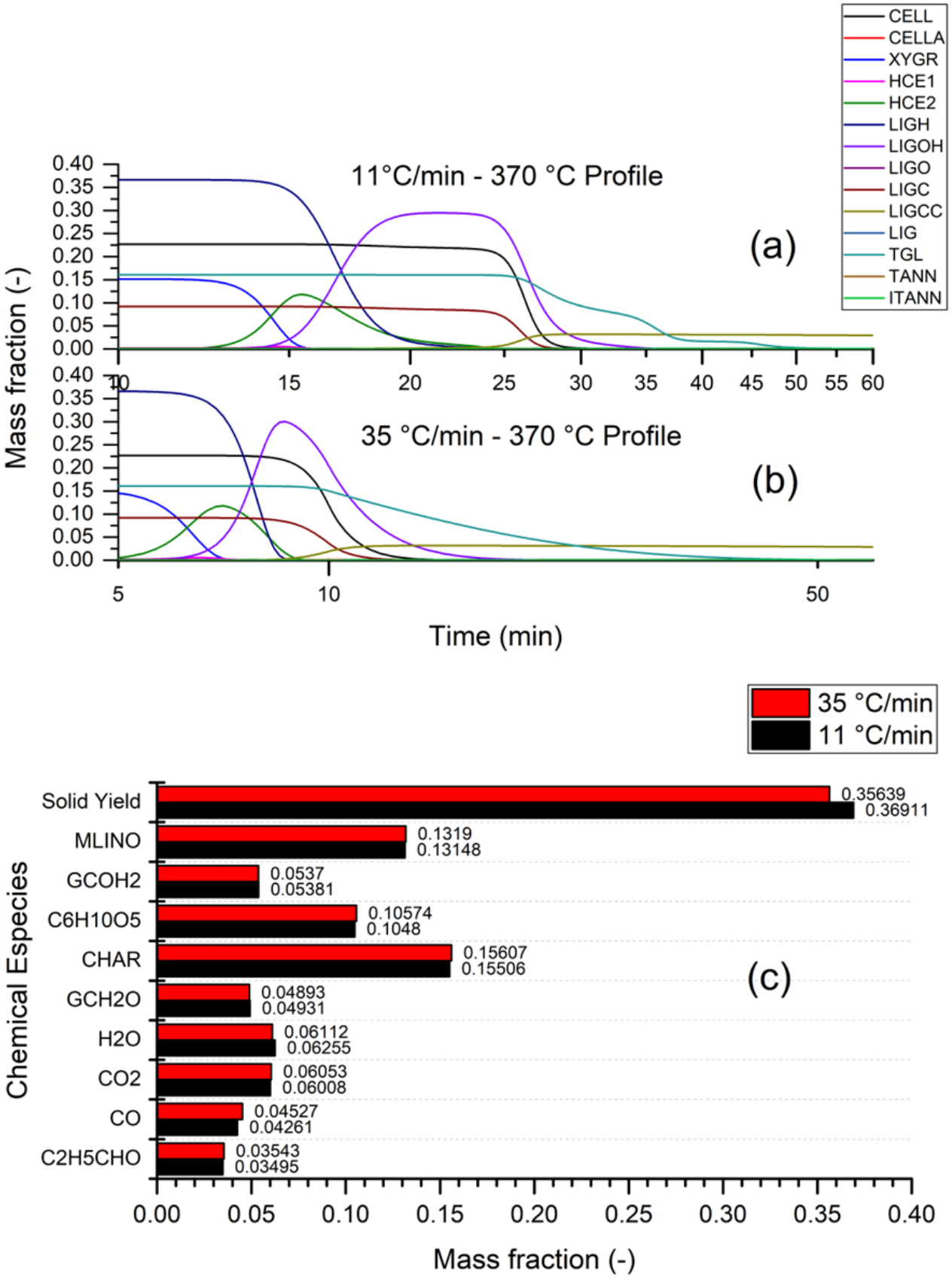

Source: The Authors.

3.4 BIOCHAR CHARACTERIZATION

3.4.1 pH, Electric conductivity (EC) and Cation Exchange Capacity (CEC)

The dry biomass contained acidic pH levels (less than 7) while both biochar samples A and B were alkaline, with pH 12.40 and 12.81, respectively. These values were higher than banana peel biochar produced in other studies, such as Feitosa *et al.* (2020) and Ali *et al.* (2019), which reported pH values of 9.4 and 10.88, respectively. The slight increase in pH from biochar A to biochar B could be attributed to the higher than the average heating profile. It was reported in Singh, Camps-Arbestain e Lehmann (2017) that there was a direct relation between pH and pyrolysis temperature but the main effect comes from the biomass itself. For example, corn straw biochar produced at 600 °C had a pH of 9.42 (Lehmann *et al.*, 2011) while banana peel biochar produced at 350 °C had a pH of 10.88 (Ali *et al.*, 2019). On the other hand, (Souza, 2019) compared pH values of biochar produced from the same biomass at temperatures of 350 and 450 °C and reported a difference of 1.3. Additionally, the high pH value of the produced biochar may be attributed to the ash content in biomass (approximately 15% wt, d.b.). This is a result of functional acid groups decomposing and leaving behind alkaline and alkaline earth salts. Consequently, low ash content biochars usually have a lower pH than higher ash content biochars (Ok *et al.*, 2015; Singh; Camps-arbestain; Lehmann, 2017).

In general, high pH biochars are relevant for applications as amendment in acidic soils ("liming effect"). Hale *et al.* (2020) observed that this application was able to counteract soil issues such as phosphorous (P) deficiency and the negative effects related to the presence of Al. However, a caveat was also noted in that a too high pH can result in less C stability in the soil and was associated with micronutrient deficiency and reduced crop yields. Electrical conductivity presents the same trend as pH and increases with respect to temperature. EC peak values were 17.22 $mS\,cm^{-1}$ and 17.87 $mS\,cm^{-1}$ for biochars A and B, respectively. These values were within the range found in other studies of banana peel biochar (12 to 20 $mS\,cm^{-1}$) and was related to the amount of soluble salts present in the biomass (Feitosa *et al.*, 2020).

Biochar CEC was determined from a sample containing both biochar A and B due to the relatively large amount required to perform the test and the small yield of each individual sample. Results are presented in Tab. 4 along with pH and EC of biochar produced from other biomasses for comparison purposes. The measured CEC value of 511 $mmol\,kg^{-1}$ in this study is considerably higher than those from other biochars found in reference works with the exception of corn straw and rice husk (Purakayastha; Kumari; Pathak, 2015). Table 4 also demonstrates that the type of biomass has a larger influence on CEC than any other parameter, followed somewhat by pH. Brady and Weil (2013) noted that increased biochar pH rised the negative charge of some silicious clay and the amount of Al and Fe oxides, all of which could increase CEC. Thus, the high pH values measured in this study could have influenced CEC directly. The CEC value of this study also exceeds the minimum value of 200 $mmol\,kg^{-1}$ recommended in Brazilian agricultural legislation (MAPA No. 35, dated July 4, 2006) (Ministério da Agricultura, Pecuária e Abastecimento, 2006), which is used as a potential indicator of the suitability of biochar as a soil amendment (Ministério da Agricultura, Pecuária e Abastecimento, 2006).

Table 4 – Comparison of pH, EC and CEC obtained in this study and reference values.

Biomass	Heating profile	pH	Electrical conductivity ($mS\,cm^{-1}$)	CEC ($mmol\,kg^{-1}$)	CEC Method	Source
Dry banana peel	–	5.17	12.33	–	Calcium acetate	Present study
Biochar A	370 °C	12.40	17.22	511	Ammonium acetate	Present study
Biochar B	370 °C	12.81	17.87	58.7	Ammonium acetate	(Lehmann *et al.*, 2011)
Chicken manure	600 °C	10.33	–	252	Ammonium acetate	–
Corn straw	600 °C	9.42	–	44.6	Ammonium acetate	J. W. Gaskin et al. (2008)
Peanut shell	400 and 500 °C	9.96	–	635	Ammonium acetate	Purakayastha et al. (2015)
Corn straw	400 °C	10.7	3.84	973	Ammonium acetate	–
Rice husk	400 °C	8.6	7.68	43	Calcium acetate	(Souza, 2019)
Rice husk	350 °C	6.4	–	47	–	–
Rice husk	450 °C	7.7	–	–	–	(Ali *et al.*, 2019)
Banana peel	350 °C	10.88	20.52	–	–	(Feitosa *et al.*, 2020)
Banana peel	400 °C	9.4	12.67	–	–	–
Orange peel	400 °C	10.1	1.8	4.19	Point of zero net charge method (Zelazny; He; Vanwormhoudt, 2018)	(Inyang *et al.*, 2010)
Sugarcane bagasse	600 °C	7.7	–	296	–	SILVA (2017)
Coffee straw	350 °C	8.94	–	296	–	–
Eucalyptus bark	350 °C	7.20	–	99.2	–	–

Source: The Authors.

3.4.2 Density, specific surface area and morfology

Results show that there was little change in the density even after undergoing thermochemical conversion regardless of the heating profile used. The measured values were 1.4234, 1.4208 and 1.4305 $g\,cm^{-3}$ for dry banana peel, biochar A and biochar B, respectively. The specific surface area was measured only for dry banana peel and biochar B produced with a heating rate of 35 °C/min. Measured values were 0.1423 and 2.4013 $m^2\,g^{-1}$, respectively. The increase in temperature resulted in a significant increase in this parameter about 17%. This suggested a direct relation between the specific surface area of the biochar and pyrolysis temperature. A reference study produced banana peel biochar at temperatures of 300, 400 and 500 °C which resulted in specific surface areas of 8, 28 and 51 $m^2\,g^{-1}$, respectively (Shiung *et al.*, 2018). These values were much higher than 2.4013 $m^2\,g^{-1}$ obtained in this study and might be related to temperature effects. On the other hand, another study converted banana peel into biochar with an elevated temperature (600 °C) and obtained a relatively low specific surface area of 11.32 $m^2\,g^{-1}$ (Kim *et al.*, 2020).

Shiung *et al.* (2018) suggested that increases in specific surface area were due to the release of volatile substances and the formation of pores in the solid, which naturally tended to rise as temperature increased. This result was confirmed in SEM scans of the biochar produced in this study presented in Fig. 5(a-f). Dry banana peel images are shown in Fig. 5(a-b) while biochar A images are shown in Fig. 5(c-f). The images show a honeycomb-shaped structure with pores range from 22.86 to 55.62 μm in diameter, which was similar to reported values from other studies (Branca; Blasi, 2015; Shiung *et al.*, 2018). High porosity and pore volume could be favorable to the adsorption of organic carbon. This stimulates microorganisms in the soil and may have other applications, such as water retention increase (Ali *et al.*, 2019; Bediako *et al.*, 2019; Kim *et al.*,

2020; Ok *et al.*, 2015; Xue *et al.*, 2019).

Figure 5 – SEM images showing the morphology of banana peel (a, b) and biochar A (c – f).

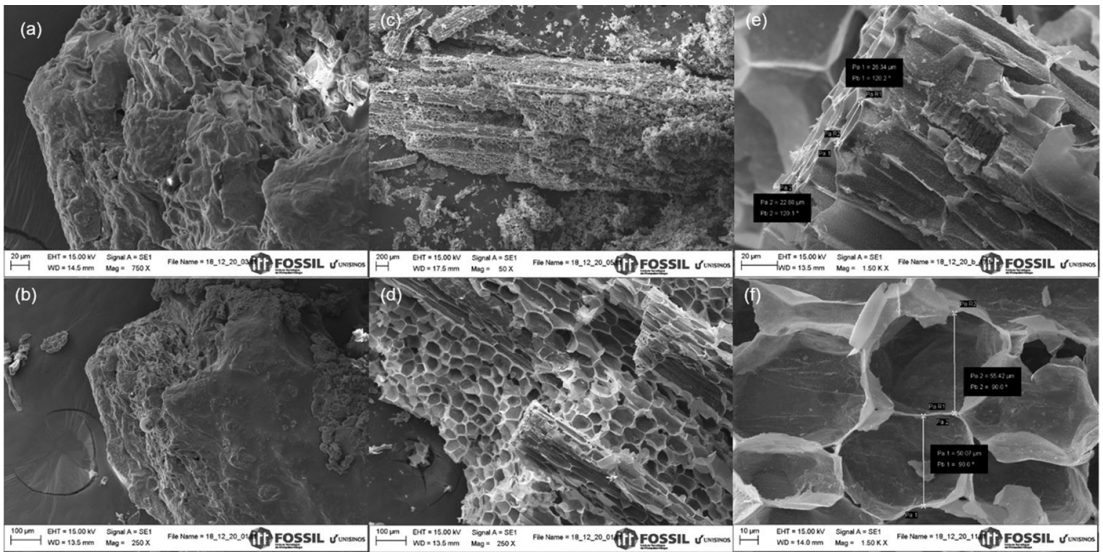

Source: The Authors.

3.4.3 C/N, H/C and O/C ratios and biochar yield

Table 5 shows the results from ultimate analysis of banana peel and biochar produced, as well as the atomic ratios and biochar yield. There is a tendency of increased C content in biochar samples when compared to the banana peel with a peak of 54.08% w.t. for biochar A. This result agrees with biochar produced at the same temperature by Shiung et al. (2018), which also noted a decrease in H content. While biochar A had an increase of almost 6% in carbon content with respect to the banana peel, biochar B, despite being produced at the same pyrolysis temperature, increased the carbon content by only 0.34%.

The small increase in carbon content of biochar B might be a result of the higher heating rate in the heating profile. This trend would lead to a shorter heating time and a non-uniform heat distribution in the biomass within the reactor. Thus, portions of the solid biomass would not undergo conversion within the chosen experimental time. Wang *et al.* (2020) analyzed factors affecting heating time in the pyrolysis of corn straw, wheat straw and peanut shell. It was determined that mineral content in biochar was affected by the type of biomass, heating time and temperature along with C, K and Ca contents. An example of this complex interaction was observed in this study as biochar samples A and B had solid yields of 36.90% and 41.68%, respectively (around 5%) based on variations of the heating profile. When compared to the simulations, biochar A had nearly matching yields: 36.91% and 36.90% for simulation and experiment, respectively. However, the discrepancy with respect to biochar B increased to 6.05%.

Table 5 shows that the atomic ratios of H/C and O/C in both biochar samples A and B were lower than in the dry banana peel. This indicated higher O and H loss compared to C with the release of volatiles during

conversion (Crombie *et al.*, 2013). In particular, biochar A had the lowest H/C and O/C ratios which indicated increased stability and aromatic content of this material with respect to the banana peel and biochar B (Crombie *et al.*, 2013; Ok *et al.*, 2015).

Table 5 – Results of elemental analysis; C/N, H/C and O/C ratios and biochar yield.

Type	Dry banana peel	Biochar A	Biochar B
C (% wt) db	48.13	54.08	48.47
H (% wt) db	5.79	4.42	4.36
O* (% wt) db	29.08	24.53	28.93
N (% wt) db	1.21	1.19	1.48
S (% wt) db	0.14	0.13	0.11
C/N	39.77	45.44	33.42
H/C	0.12	0.08	0.09
O/C	0.60	0.45	0.59
Yield	100%	36.90%	41.68%

Source: The Authors.

This characteristic can be analyzed through the Van Krevelen diagram of Fig. 6a. In this figure, the results from this study are compared with reference work, noting that biomasses closer to the origin tend to be more recalcitrant. In Fig. 6a, due to their lower atomic ratios, biochar A and B are shown to be more stable and recalcitrant to degradation than biochars from other banana peel (Ali *et al.*, 2019; Shiung *et al.*, 2018), pinus (Nanda *et al.*, 2013), wheat straw (Kwoczynski, 2021), olive oil pressing bagasse (El-bassi *et al.*, 2021) and corn straw (Ruzickova *et al.*, 2021). Only rice husk and chicken manure biochar (Nsamba *et al.*, 2015; Rodriguez *et al.*, 2020) had similar ratios as the biochars of this study.

Biochar recalcitrance to degradation is directly related to soil carbon sequestering capacity, which prevents CO_2 release to the atmosphere. Yang *et al.* (2021) estimated that 337.83 kg of biochar applied per tonnage of crop residue could retain 4.50% of all CO_2 emissions emitted in China yearly. Xu *et al.* (2020) also noted an increase of 490% in carbon retention with biochar from bamboo pyrolysis produced at 500 °C applied at a ratio of 5 ton/ha. Similarly, Yang *et al.* (2020) reduced soil CO_2 emissions by 25% with biochar from corn crop residue produced at 500 °C and applied at a ratio of 15 ton/ha.

Figure 6b presents measured C/N ratios of the biochars produced in this study and reference values. Measured C/N ratio increased from 39.77% for banana peel to 45.44% for biochar A and decreased to 33.42% for biochar B. The reduction in C/N for biochar B was due to the increase in concentration of N with respect to the increase in C in the conversion process. However, these values are considered within the range of values observed for other biochars in other studies shown in Fig. 6b. Also, it seems to exist a relation between high C/N values and soil microorganism ability to lock N, increasing its availability (Ok *et al.*, 2015).

Figure 6 – Van Krevelen diagram of H/C to O/C ratio of several biomasses.

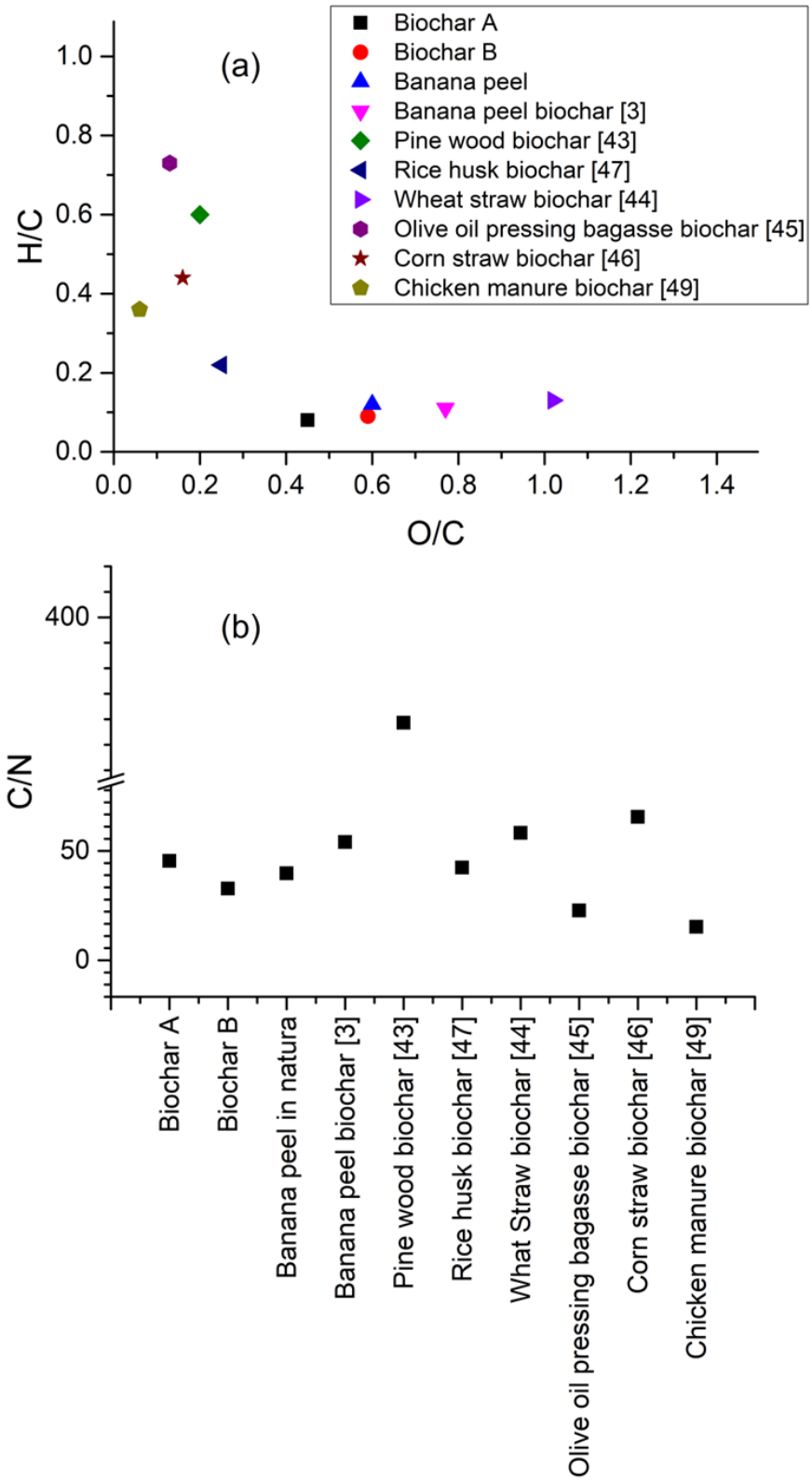

Source: The Authors.

4 CONCLUSIONS

As the computational model used in this study was shown to be an auxiliary tool to predict the decomposition of lignocellulosic structures and the effect of pyrolysis conditions in the final product. Measured values of pH in the biochars indicated a highly alkaline structure followed by a high cation exchange capacity, suggesting a potential use as a soil additive and in acidic soils as an amendment. Also, biochars A and B proved to be more stable and recalcitrant to degradation than biochars from other biomasses. Overall, the characteristics found in the produced biochars demonstrated viable application in agricultural soils as an amendment.

REFERENCES

Ali, T. *et al.* Contrasting effects of banana peels waste and its biochar on greenhouse gas emissions and soil biochemical properties. **Process Safety and Environmental Protection**, v. 122, p. 366–377, 2019.

ASTM. **Standard Test Method for Gross Calorific Value of Refuse-Derived Fuel by the Bomb Calorimeter**. 2004.

Basu, P. **Biomass Gasification, Pyrolysis and Torrefaction**. [S.l.: s.n.], 2008.

Bediako, J. K. *et al.* Characterization of the residual biochemical components of sequentially extracted banana peel biomasses and their environmental remediation applications. **Waste Management**, v. 89, p. 141–153, 2019.

Branca, C.; Blasi, C. D. A lumped kinetic model for banana peel combustion. **Thermochimica Acta**, v. 614, p. 68–75, 2015.

Brasil. **Instrução Normativa nº 17**. 2007.

Bruckman, V. J. *et al.* **Biochar - A Regional Supply Chain Approach in View of Climate Change Mitigation**. [S.l.]: Cambridge University Press, 2016.

Chen, D. *et al.* Investigation of biomass torrefaction based on three major components: Hemicellulose, cellulose, and lignin. **Energy Conversion and Management**, v. 169, p. 228–237, 2018.

Crombie, K. *et al.* The effect of pyrolysis conditions on biochar stability as determined by three methods. **GCB Bioenergy**, v. 5, p. 122–131, 2013.

Debiagi, P. *et al.* A predictive model of biochar formation and characterization. **Journal of Analytical and Applied Pyrolysis**, v. 134, p. 326–335, 2018.

Eduardo, P. *et al.* Extractives extend the applicability of multistep kinetic scheme of biomass pyrolysis. **Energy & Fuels**, 2015.

El-bassi, L. *et al.* Application of olive mill waste-based biochars in agriculture: Impact on soil properties, enzymatic activities and tomato growth. **Science of the Total Environment**, v. 755, p. 142531, 2021.

Emaga, T. H. *et al.* Effects of the stage of maturation and varieties on the chemical composition of banana and plantain peels. **Food Chemistry**, v. 103, p. 590–600, 2007.

Feitosa, A. A. *et al.* Characterization of biochar samples of banana peels and orange bagasse carbonized at 400 and 600°c. **Revista Virtual de Química**, v. 12, p. 901–912, 2020.

Hale, S. E. *et al.* The effect of biochar, lime and ash on maize yield in a long-term field trial in a ultisol in the humid tropics. **Science of the Total Environment**, v. 719, p. 137455, 2020.

Inyang, M. *et al.* Biochar from anaerobically digested sugarcane bagasse. **Bioresource Technology**, v. 101, p. 8868–8872, 2010.

Kim, H. *et al.* Removal efficiencies of manganese and iron using pristine and phosphoric acid pre-treated biochars made from banana peels. 2020.

Kwoczynski, Z. Characterization of biomass wastes and its possibility of agriculture utilization due to biochar production by torrefaction process. **Journal of Cleaner Production**, v. 280, 2021.

Lehmann, J. *et al.* Biochar effects on soil biota - a review. **Soil Biology and Biochemistry**, v. 43, p. 1812–1836, 2011.

Leobet, J. **Casca de banana (Musa cavendishii) como fonte de energia e caracterização do resíduo mineral fixo**. 2016. Dissertação (Mestrado) — Universidade Federal de Santa Catarina, 2016.

Loo, S. v.; Koppejan, J. (Ed.). **The Handbook of Biomass Combustion and Co-firing**. London: Earthscan, 2008.

Meena, R. S. **Soil Health Restoration and Management**. [S.l.: s.n.], 2020.

Ministério da Agricultura, Pecuária e Abastecimento. **Instrução Normativa nº 35**. 2006.

Motghare, K. A. *et al.* Comparative study of different waste biomass for energy application. **Waste Management**, v. 47, p. 40–45, 2016.

Nanda, S. *et al.* Characterization of north american lignocellulosic biomass and biochars in terms of their candidacy for alternate renewable fuels. **BioEnergy Research**, v. 6, p. 663–677, 2013.

Nathoa, C.; Sirisukpoca, U.; Pisutpaisal, N. Production of hydrogen and methane from banana peel by two phase anaerobic fermentation. **Energy Procedia**, v. 50, p. 702–710, 2014.

Naydenova, I. *et al.* Pollutants formation during single particle combustion of biomass under fluidized bed conditions: An experimental study. **Fuel**, v. 278, p. 117958, 2020.

Novotny, E. H. *et al.* Biochar: Carbono pirogênico para uso agrícola - uma revisão crítica. **Revista Brasileira de Ciência do Solo**, v. 39, p. 321–344, 2015.

Nsamba, H. K. *et al.* Designing and performance evaluation of biochar production in a top-lit updraft up-scaled gasifier. **Journal of Sustainable Bioenergy Systems**, v. 5, p. 41–55, 2015.

Ok, Y. S. *et al.* (Ed.). **Biochar: Production, Characterization and Applications**. [S.l.]: CRC Press, 2015.

Omulo, G. *et al.* Optimizing slow pyrolysis of banana peels wastes using response surface methodology. v. 24, p. 354–361, 2019.

Purakayastha, T. J.; Kumari, S.; Pathak, H. Characterisation, stability, and microbial effects of four biochars produced from crop residues. **Geoderma**, v. 239–240, p. 293–303, 2015.

Ralebitso-senior, T. K.; Orr, C. H. **Biochar Application: Essential Soil Microbial Ecology**. [S.l.: s.n.], 2016.

Rodriguez, J. A. *et al.* Influence of pyrolysis temperature and feedstock on the properties of biochars produced from agricultural and industrial wastes. **Journal of Analytical and Applied Pyrolysis**, v. 149, p. 104839, 2020.

Ruzickova, J. *et al.* A comprehensive assessment of potential hazard caused by organic compounds in biochar for agricultural use. **Journal of Hazardous Materials**, v. 403, p. 123644, 2021.

Shiung, S. *et al.* Pyrolysis production of fruit peel biochar for potential use in treatment of palm oil mill effluent. **Journal of Environmental Management**, v. 213, p. 400–408, 2018.

Singh, B.; Camps-arbestain, M.; Lehmann, J. **Biochar: A Guide to Analytical Methods**. [S.l.]: CSIRO Publishing, 2017.

Souza, D. M. d. **Avaliação das propriedades do biocarvão obtido por carbonização a partir de cascas de arroz, visando sua aplicação em solos agrícolas**. 2019. Dissertação (Mestrado) — Universidade do Vale do Rio dos Sinos, 2019.

Souza, O. *et al.* Energia alternativa de biomassa: Bioetanol a partir da casca e da polpa de banana. **Revista Brasileira de Engenharia Agrícola e Ambiental**, v. 16, p. 915–921, 2012.

Tahir, M. H. *et al.* Thermo-kinetics and gaseous product analysis of banana peel pyrolysis for its bioenergy potential. **Biomass and Bioenergy**, v. 122, p. 193–201, 2019.

Vassilev, S. V. *et al.* An overview of the chemical composition of biomass. **Fuel**, v. 89, p. 913–933, 2010.

Wang, S. *et al.* Influence of temperature and residence time on characteristics of biochars derived from agricultural residues: A comprehensive evaluation. **Process Safety and Environmental Protection**, v. 139, p. 218–229, 2020.

Xu, L. *et al.* Biochar application increased ecosystem carbon sequestration capacity in a moso bamboo forest. **Forest Ecology and Management**, v. 475, p. 118447, 2020.

Xue, M. *et al.* Optimized synthesis of banana peel derived porous carbon and its application in lithium sulfur batteries. **Materials Research Bulletin**, v. 112, p. 269–280, 2019.

Yang, Q. *et al.* Country-level potential of carbon sequestration and environmental benefits by utilizing crop residues for biochar implementation. **Applied Energy**, v. 282, p. 116275, 2021.

Yang, W. *et al.* Impact of biochar on greenhouse gas emissions and soil carbon sequestration in corn grown under drip irrigation with mulching. **Science of the Total Environment**, v. 729, p. 138752, 2020.

Zelazny, L. W.; He, L.; Vanwormhoudt, A. Charge analysis of soils and anion exchange. In: . [S.l.: s.n.], 2018. p. 1231–1253.